ELSEVIER

S0032-3861(96)00485-5

Polymer Vol. 38 No. 1, pp. 35–42, 1997

0032-3861/97/$17.00 + 0.00

Low-molar-mass cyclic poly(oxyethylene)s studied by Raman spectroscopy, X-ray scattering and differential scanning calorimetry

Ga-Er Yu*, Tao Sun, Ze-Gui Yan, Colin Price and Colin Booth
Manchester Polymer Centre, Department of Chemistry, University of Manchester, Manchester M13 9PL, UK

and Jennifer Cook and Anthony J. Ryan†
Manchester Materials Science Centre, UMIST, Grosvenor Street, Manchester M1 7HS, UK and †CLRC, Daresbury Laboratory, Warrington WA4 4AD, UK

and Kyriakos Viras
National and Kapodistrian University of Athens, Department of Chemistry, Physical Chemistry Laboratory, Panepistimiopolis, 157 71 Athens, Greece
(Received 13 February 1996; revised 26 March 1996)

Crystalline cyclic poly(oxyethylene)s of number-average molar mass 1000, 1500, 2000 and 3000 g mol^{-1} were studied by high-frequency and low-frequency laser-Raman spectroscopy, wide-angle (WAXS) and small-angle (SAXS) X-ray scattering, and differential scanning calorimetry (d.s.c.). Comparison was made with the properties of corresponding linear poly(oxyethylene) dimethyl ethers. The crystal structures of the linear and cyclic polymers were essentially the same as that of high-molar-mass poly(oxyethylene). The cyclic polymers crystallized in the twice-folded conformation and the linear polymers in the extended conformation, as confirmed by their lamellar spacings (SAXS) and the frequencies of their single-node longitudinal acoustic modes (LAM-1). Compared at identical lamellar spacing, the cyclic polymers had identical enthalpies of fusion (per mol of chain units) as the linear polymers but higher melting temperatures, consistent with lower entropies of fusion (per mol of chain units) for the cyclic polymers. Copyright © 1996 Elsevier Science Ltd.

(Keywords: crystalline; cyclic; poly(oxyethylene))

INTRODUCTION

Comparative studies of the structures of crystalline linear and cyclic polymers are not common. Attention has been directed mainly towards cyclic oligomers: examples are studies by Wegner and coworkers[1–3] of linear and cyclic alkanes, and by Höcker and coworkers[4] of linear and cyclic oligourethanes. In spite of recent interest[5–7] in the preparation of cyclic oligo(oxyethylene)s, i.e. large crown ethers, no systematic study of their crystallinity has been reported.

The crystallinity of low-molar-mass linear poly(oxyethylene)s is well documented: e.g. studies by X-ray scattering[8,9], differential scanning calorimetry[10,11], and Raman spectroscopy[12–14]. This activity has owed much to the ready availability, from a number of manufacturers, of polyethylene glycols [α-hydro, ω-hydroxy-poly(oxyethylene)s] with narrow molar mass distributions (often $M_w/M_n \leq 1.1$) and number-average molar masses (M_n) up to 20 000 g mol^{-1}. Specific effects of chain length on crystallinity, particularly on chain folding, are well understood. The present interest in cyclic poly(oxyethylene)s can be judged against this background.

A comparative study of crystalline cyclic and linear poly(oxyethylene)s was reported recently[15]. The cyclic polymers were prepared[16] from polyethylene glycols by reaction with dichloromethane, ring closure being affected by the formation of an acetal link:

$$\left[\text{OCH}_2(\text{OCH}_2\text{CH}_2)_m\right]$$

The precursor polymers had narrow molar mass distributions and number-average molar masses (M_n) in the range of 1000–3000 g mol^{-1} (i.e. number-average $m \approx 23$–68, equivalent to 69–204 chain atoms). These characteristics carried through to the cyclic polymers. Low-frequency Raman spectroscopy was used to determine single-node longitudinal acoustic mode (LAM-1) frequencies. High-frequency Raman spectroscopy served to define chain conformation and packing[15]. It was confirmed that the cyclic polymers crystallized in the usual way[17], i.e. as alternate right- and left-handed

* To whom correspondence should be addressed

helices forming a monoclinic sub-cell. However, they are necessarily crystallized in a twice-folded conformation, as indicated schematically below.

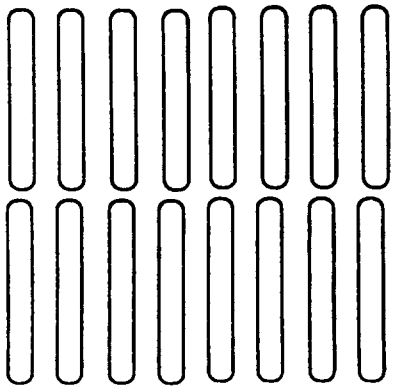

The work reported in this paper adds to the previous study[15] in a number of ways.

(i) The range of cyclic poly(oxyethylene)s used was extended to include rings closed by ether linkage

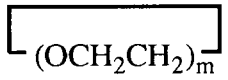

As described below, this additional work showed that the crystallinity of the cyclic poly(oxyethylene)s was not significantly affected by the presence of one non-crystallizable acetal linkage.

(ii) X-ray scattering (wide-angle, WAXS, and small-angle, SAXS) patterns were obtained for all samples. This was in addition to high- and low-frequency Raman spectra and differential scanning calorimetry (d.s.c.) curves, as obtained previously[15]. These new observations confirmed beyond doubt the crystal structure and morphology of the cyclic polymers.

(iii) Poly(oxyethylene) dimethyl ethers, [α-methyl, ω-methoxy-poly(oxyethylene)s] prepared from the same precursor glycols as the cyclic polymers were investigated by the same techniques. Previously[15] only the precursor glycols had been studied. The effect of hydroxy end groups (compared to methyl end groups) on the LAM-1 of a short poly(oxyethylene) chain can be significant (e.g. a difference of 10% for $M_n = 2000\,g\,mol^{-1}$)[13]. The new measurements proved a better basis for comparing the LAM-1 frequencies of the cyclic and linear polymers.

EXPERIMENTAL

Preparation and characterization

Cyclic and methyl-ended poly(oxyethylene)s were prepared (from commercial polyethylene glycol precursors) and purified as described previously[16;18–20]. All methods involved a Williamson ether synthesis carried out in the presence of powdered KOH. Reaction at extreme dilution of a polyethylene glycol with either dichloromethane or tosyl chloride resulted in high conversion (*ca* 90%) to a cyclic poly(oxyethylene) closed by either an acetal or an ether group[16,18]. Cyclic polymer was efficiently separated from chain-extended byproducts through difference in solubility. Reaction of a polyethylene glycol with iodomethane gave practically complete conversion (> 99%) to the dimethyl ether[19,20].

N.m.r. spectra were recorded by means of a Varian Unity 500 spectrometer operated at 500 MHz for ^1H or 125 MHz for ^{13}C spectra, using solutions of *ca* 5 wt% in $CDCl_3$. The number-average molar masses (M_n) of the linear dimethyl ethers and the cyclics with acetal closure were checked and found to be essentially identical (within an experimental uncertainty of ±5%) with those of the precursor glycols. Since the values obtained closely corresponded to the manufacturer's specifications, their rounded values (i.e. M_n = 1000, 1500, 2000 and 3000 $g\,mol^{-1}$) were adopted. Because of their uniformity of composition, the cyclic polymers with ether closure could not be characterized in this way, apart from checking that their n.m.r. spectra contained single peaks at 3.6 ppm (^1H) or 70.3 ppm (^{13}C). However, as discussed previously[18] and shown again below, characterization of the solid state by SAXS and low-frequency Raman spectroscopy yielded results which were entirely consistent with all cyclics having the same number-average chains lengths as their precursors.

The g.p.c. system generally used to investigate the polymers comprised three μ-Styragel columns with porosities 500, 10^3 and 10^4 Å. The eluent was THF at 20°C and 1 $cm^3\,min^{-1}$ flow rate. A differential refractometer (Waters R410) was used to detect elution of sample. Elution volumes were referenced to dodecane as internal standard. A calibration curve has been published[18], as have examples of g.p.c. curves[16,18]. All samples were found to have predominantly narrow size distributions, with ratios of mass-average to number-average molar mass, $M_w/M_n \approx 1.05$ (without correction for instrumental spreading). Compared at the same molar mass, the cyclic polymers eluted at higher volumes than the linear polymers, consistent with a smaller coil size for the cyclic polymers[21]. Small signals on the low-elution-volume side of the main peak in the g.p.c. curves of the cyclized samples indicated the presence of chain-extended polymer (linear or cyclic) not separated by the fractionation process employed[16] in their purification, but the areas of these signals (relative to those of the main peak) were invariably small, consistent with the samples being 95–99% 'pure'.

In what follows, a given sample is denoted by its number-average molar mass and either L to signify a linear chain (followed by M for a linear dimethyl ether) or R to denote cyclic (ring), (followed by A or E to signify acetal or ether closure). Thus samples 2000L, 2000LM, 2000RA and 2000RE are, respectively, the polyethylene glycol precursor (PEG2000), its dimethyl ether, the cyclic polymer formed by acetal closure, and the cyclic polymer formed by ether closure. For convenience, the four sets of samples are referred to as series L, LM, RA and RE.

Simultaneous WAXS/SAXS

Measurements were made on beamline 8.2 of the SRS at the CCLRC Daresbury Laboratory, Warrington, UK. Details of the storage ring, radiation (λ = 1.5 Å) and

camera geometry and data collection electronics have been given elsewhere[22]. The camera was equipped with a multiwire quadrant detector (SAXS) located 3.5 m from the sample position and a curved knife-edge detector (WAXS) which covered 120° of arc at a radius of 0.3 m. A vacuum chamber placed between the sample and detectors reduced air scattering and absorption. The scattering pattern from an oriented specimen of wet collagen (rat-tail tendon) was used to calibrate the SAXS detector, and high-density polyethylene, aluminium and an NBS silicon standard were used to calibrate the WAXS detector. The experimental data were corrected for background scattering (subtraction of the scattering from the camera, hot stage and an empty cell), sample thickness and transmission, and for any departure from positional linearity of the detectors.

The specimens for SAXS/WAXS were placed in a TA Instruments DSC pan containing a 0.75 mm brass spacer ring and fitted with windows (*ca* 7 mm diameter) made from 25 μm thick mica. The loaded pans were placed in the cell of a Linkam DSC of single-pan design, which enabled samples to be melted and recrystallized *in situ*. The d.s.c. curve obtained from this system was comparable to that from a conventional, two-pan, heat-flux DSC (e.g. a Du Pont 990). A more complete description of this aspect of the apparatus can be found elsewhere[23,24]. In the present experiments, the samples taken from storage were cooled to 5 °C, melted by heating to 50–60°C at either 5 or 10 K min^{-1}, and recrystallized by cooling at 5 or 10 K min^{-1} back to 5°C. The beam-line data acquisition system had a time-frame generator programmed to collect the SAXS/WAXS data in 6 s frames separated by a wait-time of 10 μs.

For purposes of analysis, it was assumed that the samples had small domains relative to the sample size and, therefore, were isotropic with respect to the X-ray pattern: i.e. all orientations were adequately sampled in the one-dimensional experiments. Results were presented as intensity *vs* scattering angle 2θ (WAXS, normalized to Cu$K\alpha$ radiation) or intensity *vs* scattering vector $q = (4\pi/\lambda)\sin\theta$ (SAXS). Lamellar spacings (Bragg spacings) were calculated from the position (q^*) of the first-order maximum in I *vs* q, (i.e. $d = 2\pi/q^*$) and checked against the positions of well-defined higher-order maxima.

Raman spectroscopy

Raman scattering at 90° to the incident beam was recorded by means of a Spex Ramalog spectrometer fitted with a 1403 double monochromator, and with a third (1442U) monochromator operated in scanning mode. The light source was a Coherent Innova 90 argon-ion laser operated at 514.5 mm and 400 mW. Typical operating conditions for the low-frequency range under investigation were: bandwidth 1.5 cm^{-1}, scanning increment 0.05 cm^{-1}, integration time 4 s. The low-frequency scale was calibrated by reference to the 9.6 and 14.9 cm^{-1} bands in the low frequency spectrum of L-cystine. High frequency spectra were also recorded for each sample. These spectra were taken before and after recording the low-frequency spectra, and served to confirm the stability of the samples under the conditions of experiments, as well as giving useful structural information.

Samples were either enclosed in capillary tubes or were held in the hollowed end of a stainless steel rod. In either case, they were melted and cooled rapidly to room temperature to crystallize. Spectra were recorded with the samples either at a constant temperature of 15 ± 1°C (achieved by means of a Harney-Miller cell, Spex Industries Inc.) or at room temperature (20 ± 1°C). Temperature corrections between 15 and 20°C were not required, as the temperature derivative of frequency is known[13] to be small for the LAM bands of poly(oxyethylene.

Differential scanning calorimetry

A Perkin-Elmer DSC-4 was used. Known weights (< 10 mg) of the samples, which had been stored either at room temperature or in a freezer at −10°C, were sealed into aluminium pans. Samples with low melting points were cooled to 0°C in the calorimeter before heating. All samples were heated at 2 K min^{-1} through the melting point to 70–80°C, the sample rapidly cooled to a temperature well below the melting point, and the heating process repeated.

Values of the enthalpy of fusion were obtained from peak areas, and melting points were obtained from the temperature at the maximum of the peak. The power and temperature scales of the calorimeter were calibrated against the enthalpies of fusion and melting temperatures of indium, *n*-docosane, and polyethylene glycol 2000L itself, the latter being used to ensure approximate correspondence with the results reported previously[15].

RESULTS AND DISCUSSION

Samples of series L (linear hydroxy-ended) and RA (cyclic with acetal closure) have been investigated previously[15]. For this investigation, certain RA samples were resynthesized from the same (or closely related) polyethylene glycol precursors (series L), and all samples were investigated by X-ray scattering. The Raman spectroscopy of series L and RA was not repeated, and the results described and discussed below are taken from ref. 15. To ensure comparability of results, all L and RA polymers were re-examined by d.s.c., and were found to be identical within experimental error. The samples of series LM and RE, and all the results pertaining thereto are new.

Crystal structure

Both high-frequency Raman spectroscopy and WAXS showed that all samples had the same underlying crystal structure characteristic of crystalline poly(oxyethylene)[17], i.e. alternate right and left-handed helices forming a monoclinic sub-cell. The high frequency spectra recorded were similar to those published previously for poly(oxyethylene) and related oligomers[25–27], particularly in the bands at 291, 936 and 1231 cm^{-1}, which are the indicators of chain conformation and packing[26,27]. The WAXS patterns from the cyclic polymers showed similar reflections to their linear counterparts (see *Figure 1*, samples 2000RA and 2000LM) and, within the error of determination, all could be indexed by the monoclinic sub-cell[17].

Small-angle X-ray scattering

Figure 2 shows SAXS patterns for samples 3000RE and 1500LM. Pairing the SAXS results in this way provides a clear illustration of the near identity of

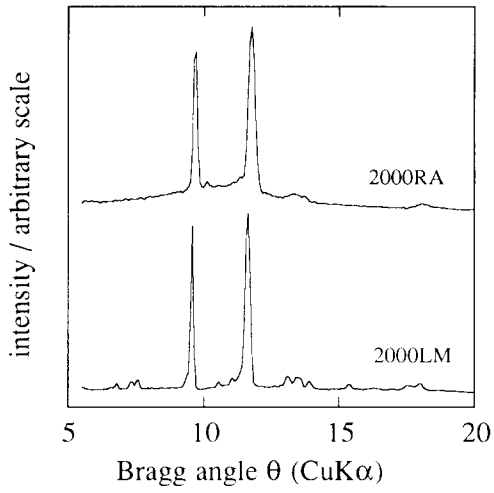

Figure 1 WAXS patterns from crystalline cyclic poly(oxyethylene) 2000RA and linear poly(oxyethylene) dimethyl ether 2000LM. The intense reflection at Bragg angle $\theta = 9.66°$ [indexed (120)] and the composite reflection at $\theta = 11.66°$ [indexed (112) and (032) among others] are characteristic of crystalline polyoxyethylene)[17]. The less intense reflections can all be indexed (to $\pm 0.1°$ in θ) by the established structure with the monoclinic sub-cell[17]. Because of operating conditions at the time, the scattering from sample 2000RA was less than one-tenth the intensity of that from sample 2000LM, with consequent loss of definition of weak reflections

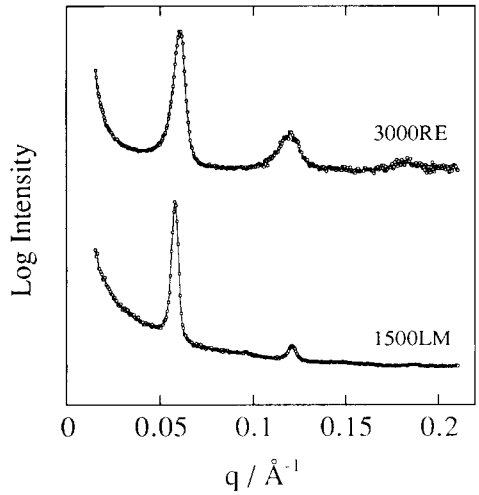

Figure 2 SAXS patterns from crystalline cyclic (3000RE) and linear (1500LM) poly(oxyethylene)s. The reflections from the lamellar spacings are at identical values of q. For clarity of presentation, the intensity scales of the two patterns are displaced relative to one another

the scattering angles of reflections from the lamellar spacings of a cyclic poly(oxyethylene) and a linear poly(oxyethylene) of half its chain length. SAXS patterns obtained for other samples were similar. The derived lamellar spacings (d) are listed in *Table 1*: the values given in parentheses are possibly affected by fractionation: see the d.s.c. results described below. The plot of d *vs* z shown in *Figure 3* [where z = number-average chain length (linear) or half-length (cyclic) in chain atoms, with allowance made for methyl and acetal groups] confirms the unfolded-chain conformation of the linear polymers and the twice-folded chain conformation of the cyclics, as shown schematically in the Introduction. The line shown in *Figure 3* is the least squares fit through the origin to all the data points, and

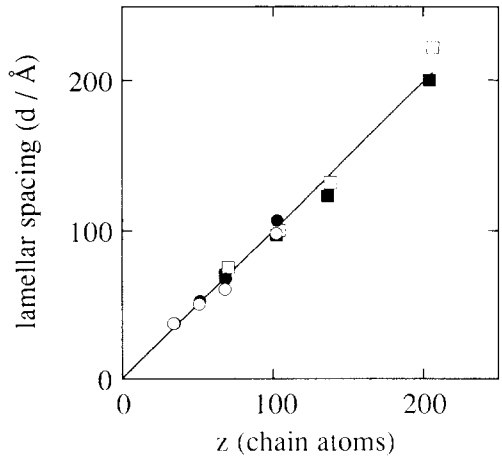

Figure 3 Lamellar spacing from SAXS *vs* z, where z = number-average chain length (linear) or half-length (cyclic) in chain atoms: (■) linear glycols (series L); (□) linear methyl ethers (series LM); (●) cyclics with acetal closure (series RA); (○) cyclics with ether closure (series RE)

corresponds to a spacing per chain atom of 0.99 ± 0.02 Å, i.e. very similar to values reported previously for the increment per chain atom along the helix axis in crystalline poly(oxyethylene)[17] (0.93 Å) and related uniform oligo(oxyethylene)s[28] (0.95 Å). This broad agreement between experiment and expectation is taken as confirmation that the cyclization and purification procedures were carried through with little or no fractionation by chain length. One reason for the slightly higher value found for the polydisperse poly(oxyethylene)s (compared to the wholly crystalline uniform oligomers[28]) could be a higher proportion of *trans* states in the emerging chain ends compared with the *trans–trans–gauche* conformation of the helical chains in the lamellar core. A second reason may be segregation of non-crystallized low-molar-mass polymer to the interlamellar region.

Thermal analysis

D.s.c. curves of the majority of samples, whether stored or recrystallized prior to heating in the DSC-4, contained single melting peaks covering a temperature range of 10 degrees or so. The d.s.c. curves of rapidly crystallized samples of 3000L and 3000LM showed evidence of chain folding, which could be removed by annealing or by crystallization at a high temperature. D.s.c. curves of rapidly-crystallized sample 3000RA showed evidence of incorporation of the acetal group, but could be annealed in the same way. These effects have been illustrated and discussed previously[15]. All samples with $M_n \approx 1000\ g\ mol^{-1}$ had low melting points ($T_m < 37°C$) and were incompletely crystalline at room temperature. Consequently, cooling these samples in the DSC prior to an experiment resulted in further crystallization, and the resulting d.s.c. curves covered a wide temperature range and contained two peaks.

Melting points and enthalpies of fusion measured for samples taken from storage are listed in *Table 1*. Because of their low melting points and wide melting ranges, satisfactory baselines were not established in the d.s.c. curves of samples with 1000RA and 1000RE, and their values of T_m and $\Delta_{fus}H$ (in parentheses in *Table 1*) are particularly uncertain. Both T_m and $\Delta_{fus}H$ were lower

Table 1 Lamellar spacing (d), LAM-1 frequencies (ν_1), melting points (T_m) and enthalpies of fusion at the metling point ($\Delta_{fus}H$) of linear and cyclic poly(oxyethylene)s[a]

Sample	d (Å)	ν_1 (cm^{-1})	T_m (°C)	$\Delta_{fus}H$ ($J\,g^{-1}$)
1000L	70	16.5	37	149
1500L	97	12.4	47	165
2000L	123	9.3	52	186
3000L	200	5.7	58	191
1000LM	75	15.4	36	150
1500LM	100	11.2	47	181
2000LM	132	9.2	51	183
3000LM	222	5.4	57	185
1000RA	(37)	(27.7)	(33)	(96)
1500RA	52	20.6	46	150
2000RA	67	16.1	51	158
3000RA	107	9.5	56	161
1000RE	(37)	(31.1)	(30)	(73)
1500RE	50	2.1	47	140
2000RE	60	18.6	52	142
3000RE	98	11.1	57	152

[a] Values of d and ν_1 for recrystallized samples; T_m and $\Delta_{fus}H$ for stored samples. Samples 3000L and 3000LM recrystallized at high temperature (or annealed) to eliminate chain folding. Reproducibilities (replicate crystallizations): d, ±5%; ν_1, ±0.2 to 1 cm^{-1} (see *Figures 6* and *7*); T_m, ±2°C; $\Delta_{fus}H$, ±10 $J\,g^{-1}$

Table 2 Effect of thermal history on the melting points (T_m) and enthalpies of fustion ($\Delta_{fus}H$) of cyclic poly(oxyethylene)s[a]

	Recrystallized		Stored	
Sample	T_m (°C)	$\Delta_{fus}H$ ($J\,g^{-1}$)	T_m (°C)	$\Delta_{fus}H$ ($J\,g^{-1}$)
1500RA	41	128	46	150
2000RA	47	141	51	158
3000RA	54	146	56	161

[a] Recrystallized samples cooled from the melt to 0°C in the DSC immediately before heating. Reproducibilities (replicate crystallizations): T_m, ±2°C; $\Delta_{fus}H$, ±10 $J\,g^{-1}$

for samples which had been recrystallized immediately before heating in the DSC. The effect could be large, as illustrated in *Table 2*. The values of T_m and $\Delta_{fus}H$ reported previously[15] for samples of series L and RA were for recrystallized samples, and so had lower values than those reported for them in *Table 1*.

A plot of melting point against reciprocal lamellar spacing is shown in *Figure 4a*. Within the experimental error (the error bars shown are ±2 degrees), and ignoring the data points for samples 1000RA and 1000RE, the melting points fall onto straight lines intercepting the ordinate at $T_m^0 \approx 69$°C. This extrapolated value is much as expected: values of T_m^0 in the range of 69–78°C have been reported previously[10,29–32], the values at the bottom end of the range being obtained using linear poly(oxyethylene)s related to those used in the present work. The extrapolation in *Figure 4a* follows the simple equation

$$T_m = T_m^0\left(1 - \frac{2\gamma}{\Delta_{fus}H^0 d}\right)$$

where γ = excess surface Gibbs energy ($J\,m^{-2}$), $\Delta_{fus}H^0$ = thermodynamic enthalpy of fusion ($J\,m^{-3}$), and d = lamellar thickness (m).

Because of the finite value of ΔC_P for poly(oxyethylene), a corresponding extrapolation of $\Delta_{fus}H$ against $1/d$ should be carried out for the enthalpy changes corrected

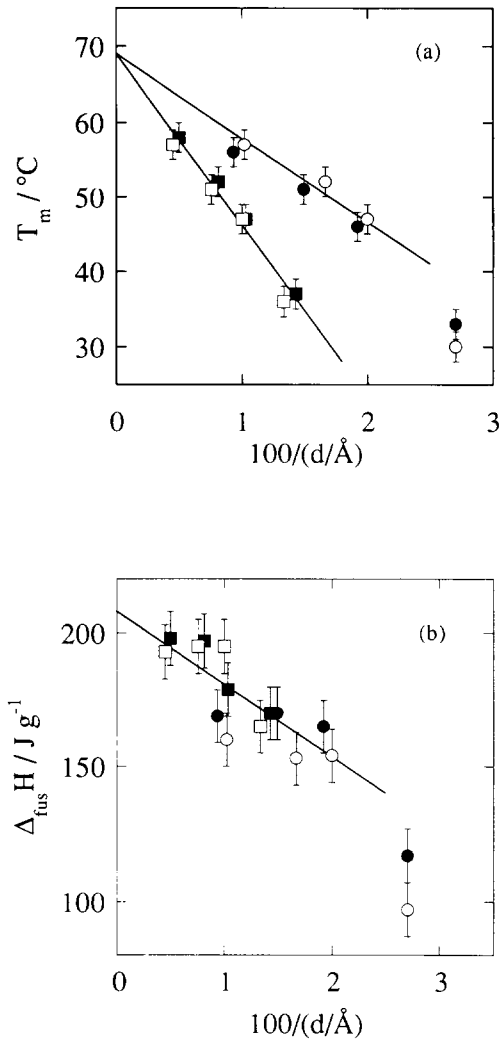

Figure 4 (a) Melting temperature and (b) enthalpy of fusion corrected to 70°C plotted against reciprocal lamellar spacing: (■) linear glycols (series L); (□) linear methyl ethers (series LM); (●) cyclics with acetal closure (series RA); (○) cyclics with ether closure (series RE). The lines are least-squares fits to the data points, the points for samples 1000RA and 1000RE being omitted

for the effect of melting temperature. The correction is[34]

$$\Delta_{fus}H(T_1) = \Delta_{fus}H(T_2) + 0.650\,(T_2 - T_1) - 0.00253\,(T_2^2 - T_1^2)$$

where temperatures are in °C. Values of $\Delta_{fus}H$ corrected to 70°C are plotted against $1/d$ in *Figure 4b*. Within a generous allowance for experimental error (the error bars shown are ±10 $J\,g^{-1}$), and ignoring the data points for samples 1000RA and 1000RE, the values for the remaining samples fall onto a single straight line, consistent with an equation of the form

$$\Delta_{fus}H = \Delta_{fus}H^0 - \frac{2\eta}{d}$$

where η is the excess surface enthalpy ($J\,m^{-2}$). The straight line intercepts the ordinate at $\Delta_{fus}H^0 \approx 208\,J\,g^{-1}$. This value is within the range of $\Delta_{fus}H^0$ values reported[10,29] for samples of this type, i.e. 197–218 $J\,g^{-1}$.

The limited range and precision of data obtained in the

present work does not encourage a more quantitative analysis, e.g. of the melting points based on the analysis of Flory and Vrij[33], as applied to low-molecular-mass polyethylene glycols by Buckley and Kovacs[10]. A major concern is the chain length distributions in the samples. The coincidence of the plots of $\Delta_{fus}H$ *vs* $1/d$ (*Figure 4b*) for the various samples indicates a similar value of the excess surface enthalpy (i.e. the enthalpy of formation of surface from perfect crystal) for both linear and cyclic polymers, which is consistent with a similarly disordered lamellar surface layer in each case. This result is consistent with the extent of crystallinity of the linear and cyclic polymers depending only on lamellar thickness, i.e. with the disordered surface layers constituting a constant fraction of the lamellar thickness. This is as expected, since the disorder originates primarily from the chain length distribution in the samples[35], and the thickness of the disordered layer is related directly to the standard deviation of the number-fraction distribution of chain length (for a linear sample) or half-chain length (for a cyclic sample). This being the case, extrapolations of the type illustrated in *Figure 4* can give only average values of γ and η, since these quantities will vary with chain length.

Given similar enthalpies of fusion, the higher melting points found for the cyclics (compared at constant lamellar spacing, see *Figure 4a*) can be attributed to lower entropies of fusion, since

$$T_m = \frac{\Delta_{fus}H}{\Delta_{fus}S}$$

This is as expected, since the linear and cyclic polymers are similarly conformationally restricted in the crystalline state but the stem of a cyclic polymer is more restricted (compared with a linear polymer of the same length) in the melt state. The common intercept for both lines in *Figure 4a* is consistent with the effect of cyclization on the entropy of fusion being negligible for extended chain crystals of very long chains.

Low-frequency Raman spectroscopy

Examples of low-frequency Raman spectra of cyclic poly(oxyethylene)s with ether closure are shown in *Figures 5* and *6*. Corresponding spectra for rings with acetal closure have been published previously[15]. The broad bands at 80 cm^{-1} are characteristic of crystalline poly(oxyethylene) and has been identified as a combination of a torsional mode of the helix[36] and a lattice mode[13]. The prominent bands at low frequencies (10–30 cm^{-1}), which vary with chain length, are assigned to LAM-1. The comparison of results for 3000RE and 1500ML made in *Figure 6* (which mirrors that made in *Figure 2*) illustrates the near identity of the LAM-1 frequencies of a cyclic poly(oxyethylene) and a linear poly(oxyethylene) of half its chain length. This result is confirmed for all the samples by the LAM-1 frequencies (ν_1) listed in *Table 1* and shown in *Figure 7*. The plot departs slightly from linearity, and a quadratic curve passing through the origin is fitted to the data. A nonlinear dependence of ν_1 on chain length has been noted previously for oligo(oxyethylene)s and explained as a result of end forces[37].

A more sensitive comparison of the LAM-1 frequencies can be made using values of $\nu_1 d$. In the absence of other effects (e.g. for chains acting as uniform rods with free ends[38]) the value of this product should be constant. Individual values of $\nu_1 d$ are rather scattered, so average values of $\nu_1 d$ are listed in *Table 3* for each series of polymers. The least certain values for samples 1000RA and 1000RE are omitted. Values of $\nu_1 z$ are included for comparison. Consideration of values of $\nu_1 d$ removes possible errors introduced by fractionation during the preparation of the cyclic polymers, while comparison

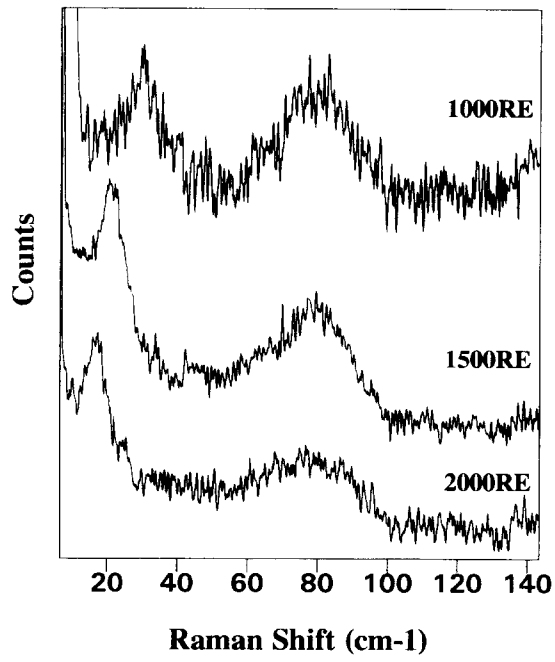

Figure 5 Low-frequency Raman spectra of cyclic poly(oxyethylene)s of series RE (as indicated). The peaks in the frequency range 18–31 cm^{-1} are assigned to LAM-1

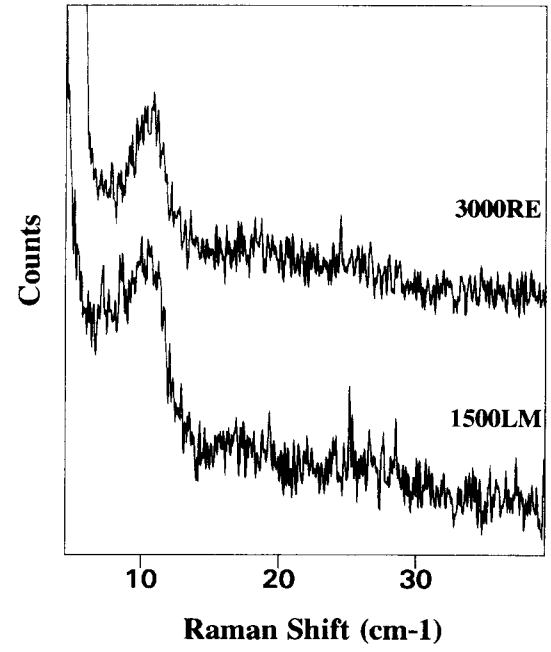

Figure 6 Low-frequency Raman spectra of cyclic poly(oxyethylene)s 3000RE and linear poly(oxyethylene) 1500LM (as indicated). The peaks at 11–12 cm^{-1} are assigned to LAM-1

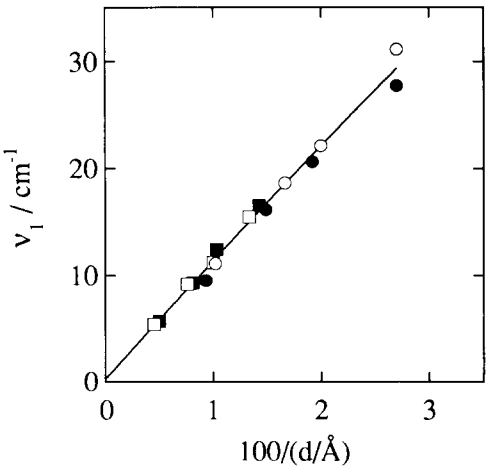

Figure 7 LAM-1 frequency (ν_1) *vs* reciprocol lamellar spacing. (■) Linear glycols (series L); (□) linear methyl ethers (series LM); (●) cyclics with acetal closure (series RA); (○) cyclics with ether closure (series RE). The curve is a least-squares-quadratic fit to all the data points

Table 3 LAM-1 frequency (ν_1) and lamellar spacing (d) for linear and cyclic poly(oxyethylene)s

Series	$\nu_1 d$ (cm^{-1} Å)	$\nu_1 z$ (cm^{-1})
L	1160 ± 30	1200 ± 80
LM	1160 ± 50	1160 ± 80
RA	1060 ± 30	1040 ± 60
RE	1100 ± 20	1180 ± 80

with linear methyl ethers removes possible effects of end association (H-bonding). Hence some of the uncertainties in our previous report[15] of the Raman spectroscopy of cyclic (series RA) and linear (series L) are not important in the present work, and the finding that the average value $\nu_1 d$ for the samples of series LM (1160 cm^{-1} Å) is higher than that for the combined series of cyclic polymers (1180 cm^{-1} Å) is satisfactorily established. It is known[37] that end forces have a significant effect on the LAM-1 frequencies of poly(oxyethylene) chains. In particular, the fractional increase in LAM-1 frequency caused by a given end force is larger the longer is the crystal stem length[37]. The effect has been demonstrated for lengthy linear and cyclic *n*-alkanes by Strobl *et al.*[39,40] and confirmed by Lee and Wegner[1]. Since the crystal stems of the linear poly(oxyethylene)s presently under discussion are systematically longer than those of the cyclic polymers, the effect of end forces will be to increase the average value of $\nu_1 d$ for the linear polymers more than for the cyclic polymers. Thus the difference (illustrated in *Table 3*) between the $\nu_1 d$ values of the linear and cyclic polymers is seen to have a straightforward explanation.

The accuracy of the present data does not allow extrapolation for comparison of LAM-1 frequency at identical lamellar thickness. The results of Lee and Wegner[1] indicate that the LAM-1 frequency is higher for a cyclic alkane compared to a linear alkane of the same chain length. A parallel investigation for linear and cyclic oxyethylene chains will require closer definition of stem length than was possible with the present non-uniform samples.

ACKNOWLEDGEMENTS

We thank Mr P. Kobryn, Mr M. Hart and Mr B. U. Komanschek for essential help with the experimental work. The Engineering and Physical Research Council, The British Council and ICI Paints Plc provided financial assistance.

REFERENCES

1 Lee, K. S. and Wegner, G. *Makromol. Chem., Rapid Commun.* 1985, **6**, 203
2 Lee, K. S., Wegner, G. and Hsu, S. L. *Polymer* 1987, **28**, 889
3 Leiser, G., Lee, K. S. and Wegner, G. *Colloid Polym. Sci.* 1988, **266**, 419
4 Heitz, W., Höcker, H., Kern, W. and Ullner, H. *Makromol. Chem.* 1971, **150**, 73
5 Chenevert, R. and D'Astous, L. *J. Heterocycl. Chem.* 1986, **23**, 1785
6 Vitali, C. A. and Masci, B. *Tetrahedron* 1989, **45**, 2201
7 Gibson, H. W., Behda, M. C., Engen, P., Shen, Y. X., Sze, J., Zhang, H., Gibson, M. D., Delaviz, Y., Lee, S. H., Liu, S., Wang, L., Nagvekar, D., Rancourt, J. and Taylor, L. T. *J. Org. Chem.* 1994, **59**, 2186
8 Arlie, J. P., Spegt, P. A. and Skoulios, A. E. *Makromol. Chem.* 1996, **99**, 160; 1967, **104**, 212
9 Spegt, P. A. *Makromol. Chem.* 1970, **140**, 167
10 Buckley, C. P. and Kovacs, A. J. *Prog. Colloid Polym. Sci.* 1975, **58**, 44
11 Buckley, C. P. and Kovacs, A. J. *Colloid Polym. Sci.* 1976, **254**, 695
12 Hartley, A. J., Leung, Y.-K., Booth, C. and Shepherd, I. W. *Polymer* 1978, **17**, 354
13 Viras, K., King, T. A. and Booth, C. *J. Polym. Sci., Polym. Phys. Ed.* 1985, **23**, 471
14 Song, K. and Krimm, S. *Macromolecules* 1990, **23**, 1946
15 Viras, K., Yan, Z.-G., Price, C., Booth, C. and Ryan, A. J. *Macromolecules* 1995, **28**, 104
16 Yan, Z.-G., Yang, Z., Price, C. and Booth, C. *Makromol. Chem., Rapid Commun.* 1993, **14**, 725
17 Takahashi, Y. and Tadokoro, H. *Macromolecules* 1973, **6**, 881
18 Sun, T., Yu, G.-E., Price, C., Booth, C., Cooke, J. and Ryan, A. J. *Polym. Commun.* 1995, **36**, 3775
19 Cooper, D. R. and Booth, C. *Polymer* 1977, **18**, 164
20 Cooper, D. R., Leung, Y.-K., Heatley, F. and Booth, C. *Polymer* 1978, **19**, 309
21 Wright, P. V. and Beevers, M. S. in 'Cyclic Polymers' (Ed. J. A. Semlyen), Elsevier, London, 1986, Ch. 3
22 Bras, W., Derbyshire, G. E., Ryan, A. J., Mant, G. R., Felton, A., Lewis, R. A., Hall, C. J. and Greaves, G. N. *Nuclear Instrum. Meth. Phys. Res*, 1993, **A326**, 587
23 Ryan, A. J. *J. Thermal Anal.* 1993, **40**, 887
24 Bras, W., Derbyshire, G. E., Clarke, S., Devine, A., Komanschek, B. U., Cooke, J. and Ryan, A. J. *J. Appl. Cryst.* 1995, **85**, 26
25 Koenig, J. L. and Angood, A. C. *J. Polym. Sci., A-2* 1970, **8**, 1787
26 Matsuura, H. and Fukuhara, K. *J. Phys. Chem*, 1987, **91**, 6139
27 Matsuura, H. *Trends Phys. Chem.* 1991, **1**, 89
28 Craven, J. R., Zhang, H. and Booth, C. *J. Chem. Soc., Faraday Trans.* 1991, **87**, 1183
29 Romankevich, O. V. and Frenkel, S. Ya. *Polym. Sci. U.S.S.R.* 1980, **22**, 2647
30 Beech, D. R. and Booth, C. *J. Polym. Sci., Part B* 1970, **8**, 731
31 Affifi-Effat, A. M. and Hay, J. N. *J. Chem. Soc., Faraday 2* 1972, **68**, 656
32 Rijke, A. M. and McCoy, S. *J. Polm. Sci., Part A-2* 1972, **10**, 1845
33 Flory, P. J. and Vrij, A. *J. Chem. Phys.* 1963, **85**, 3548
34 Campbell, C., Viras, K. Richardson, M. J., Masters, A. J. and Booth, C. *Makromol. Chem.* 1993, **194**, 799
35 Booth, C. and Colclough, R. O. in 'Comprehensive Polymer Science' (Eds C. Booth and C. Price), Pergamon Press, Oxford, 1989, Vol. 1, p. 66
36 Rabolt, J. F., Johnson, K. W. and Zitter, R. N. *J. Chem. Phys.* 1974, **61**, 504

37 Campbell, C., Viras, K. and Booth C. *J. Polym. Sci., Polym. Phys., Ed.* 1991, **29,** 1613
38 Mizushima, S. and Shimanouchi, T. *J. Am. Chem. Soc.* 1949, **71,** 1320
39 Strobl, G. R. and Eckel, F. *J. Polym. Sci., Polym. Phys. Ed.* 1976, **14,** 913
40 Tzebiatowski, T., Dräger, M. and Strobl, G. R. *Makromol. Chem.* 1982, **183,** 731